Jacek Górka, Monika Kciuk, Sebastian Stano, Szymon Domżal

Assessment of the Corrosion Resistance and the Mechanical Properties of Laser Welded Joints Made of Steel DOCOL 1200M

Abstract: The article presents test results concerning the corrosion resistance of laser beam welded joints made of steel Docol 1200m. The thickness of the joints subjected to the tests amounted to 1.8 mm. The joints were welded in the flat position (pa), without the use of the filler metal; the linear welding energy was restricted within the range of 25 J/mm to 55 J/mm. The non-destructive tests revealed that the joints represented quality level B in accordance with the ISO 13919 standard. The results of mechanical tests demonstrated the possibility of obtaining joints, the strength of which equalled that of the base material, which is unobtainable when welding such high strength steel (1200 MPa) using arc welding. The corrosion resistance tests were performed using the gravimetric method in alkaline, inert and acidic environments (0.1 M solution of sodium hydroxide (NaOH), the 3.5% solution of sodium chloride (NaCl) and the 0.1 M solution of sulphuric acid (VI) (H_2SO_4)). The material subjected to analysis was characterised by varied corrosion resistance, resulting from the test environments. The test joints contained various forms of corrosion-triggered damage including cracks, pits, swells and material losses. The above-presented corrosion resistance tests revealed that welded joints made of steel Docol 1200m were characterised by the highest corrosion resistance in the alkaline solution and the lowest corrosion resistance in the acidic solution.

Keywords: Docol 1200m, laser beam welding, corrosion resistance tests

DOI: *10.17729/ebis.2022.2/1*

Introduction

Structural steels used in civil engineering as well as in the production of vehicles and in the fabrication of pipelines and crucial structures have to satisfy strict requirements such as the appropriate value of the yield point, high weldability, high brittle crack resistance, low nil ductility transition temperature, high cold formability and relatively low manufacturing costs [1–5]. Over the past 20 years carmakers have particularly expressed their needs for steel sheets combining high strength with favourable

dr hab. inż. Jacek Górka, Professor at Silesian University of Technology in Gliwice, Department of Welding; dr inż. Monika Kciuk – Department of Engineering Materials and Biomaterials, dr inż. Sebastian Stano – Łukasiewicz Research Network – Instytut Spawalnictwa, mgr inż. Szymon Domżal – graduate of the Department of Welding, Silesian University of Technology in Gliwice;

plastic properties. The above-named needs were addressed in many international projects involving numerous companies, e.g. Ultra-Light Steel Auto Body – Advanced Vehicle Concept (Ulsab-avc) or Trailtech (by Arcelor Mittal), whose aim was to develop and manufacture components made of high-strength and plastically workable steels [6–11]. One of the results of the aforesaid efforts was the development of Advanced High-Strength Steels (ahss). These materials proved very successful in the production of vehicles because of three major factors, i.e. high tensile strength (up to 1700 MPa), a high yield point (up to 1450 MPa) and significant elongation A80 (up to 30%) [1–4]. In spite of the fact that the aforementioned steels were designed as joinable through welding, some of them still pose problems in terms of an appropriate welding method, the determination of optimum welding parameters and the ensuring of proper corrosion resistance [12–15]. For instance, significant challenges accompany the welding of martensitic steel Docol 1200m, used primarily in the production of car bumpers, side beams and other safety features of vehicles. In the above-named scope of automotive production, the process of laser welding is becoming increasingly popular. Until recently, laser welding has constituted one of many well-known and successfully applied techniques when joining simple and relatively small elements. Presently, owing to technological development and increasingly high laser power, the above-named joining technology has entered areas previously almost entirely "reserved" for conventional welding techniques [16–18]. Because of high power density obtained in areas affected by the laser beam, laser welding enables the joining of sheets (in one run) matched without square butt weld preparation, using relatively high welding rates (high efficiency).

Tests

The objective of research-related tests was to identify the corrosion resistance of 1.8 mm thick laser butt welded joints made of high-strength martensitic steel Docol 1200m. The chemical composition and mechanical properties of steel Docol 1200m are presented in Table 1, whereas the structure of the steel is presented in Figure 1.

Welding process

The tests concerning the 1.8 mm thick joints made of steel Docol 1200m welded using a TruDisk 12002 disk laser (Trumpf) were performed at Łukasiewicz Research Network – Instytut Spawalnictwa in Gliwice (Fig. 2). The welding parameters applied in the tests are presented in Table 2.

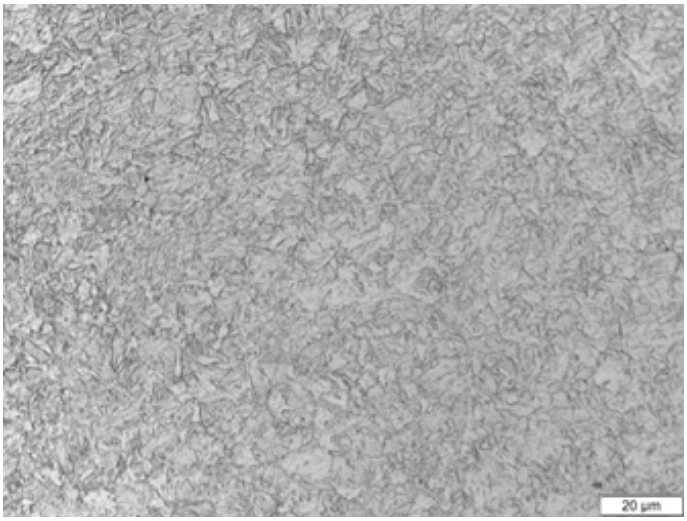

Fig. 1. Microstructure of steel DOCOL 1200M

Table 1. Chemical composition and mechanical properties of steel DOCOL 1200M

Concentration of chemical elements, %										
C	Si	Mn	P	S	Al	Nb	V	Ni	Cr	N
0.113	0.22	1.58	0.01	0.002	0.035	0.016	0.01	0.04	0.04	0.006
Mechanical properties										
Tensile strength R_m, MPa				**Yield point R_e, MPa**				**Elongation A_{80}, %**		
1260				1060				5		
* Ce – carbon equivalent according to MIS: 0.41										

Table 2. Welding parameters

Specimen designation	Power [W]	Linear energy [J/mm]	Laser beam focus diameter [mm]
1	1500	25	0.3
2	1750	35	0.3
3	2000	45	0.6
4	3500	55	0.6
Welding rate V=50 mm/s, CFO head, optical fibre (400 µm), d_{foc} = 0.6 mm, f_c = 200 mm, d_{og} = 200 mm, shielding gas: argon – 12 l/min (purity 5.0), welding without the shielding of the weld root			

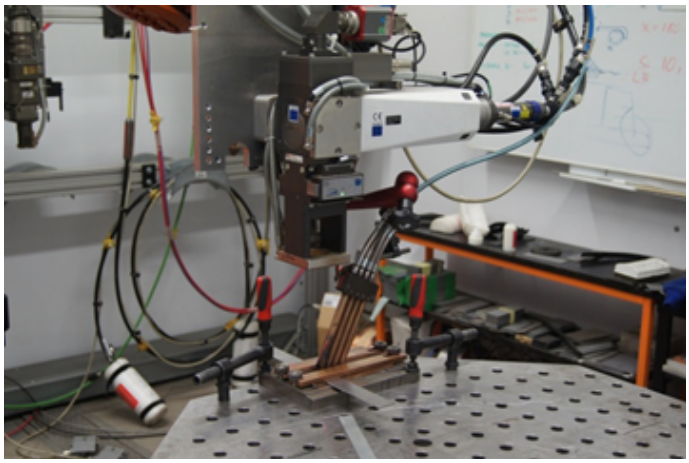

Fig. 2. Welding station

In order to determine their quality in terms of geometry and strength, the welded joints were subjected to non-destructive and destructive tests as well as to corrosion resistance tests, performed in three (i.e. alkaline, inert and acidic) environments. The results of the macro and microscopic metallographic tests are presented in Figures 3 and 4, the results of strength tests are contained in Table 3, whereas the distribution of hardness is presented in Figure 5.

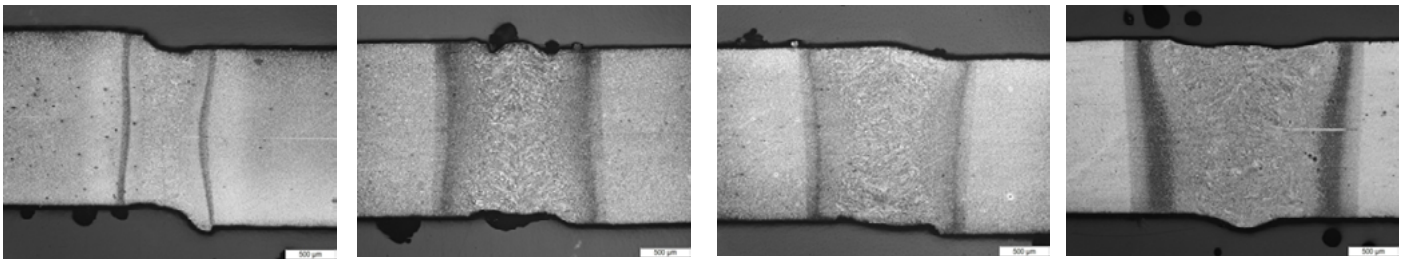

Joint 1, E = 25 J/mm | Joint 2, E = 35 J/mm | Joint 3, E = 45 J/mm | Joint 4, E = 55 J/mm

Fig. 3. Macrostructure of the welded joints

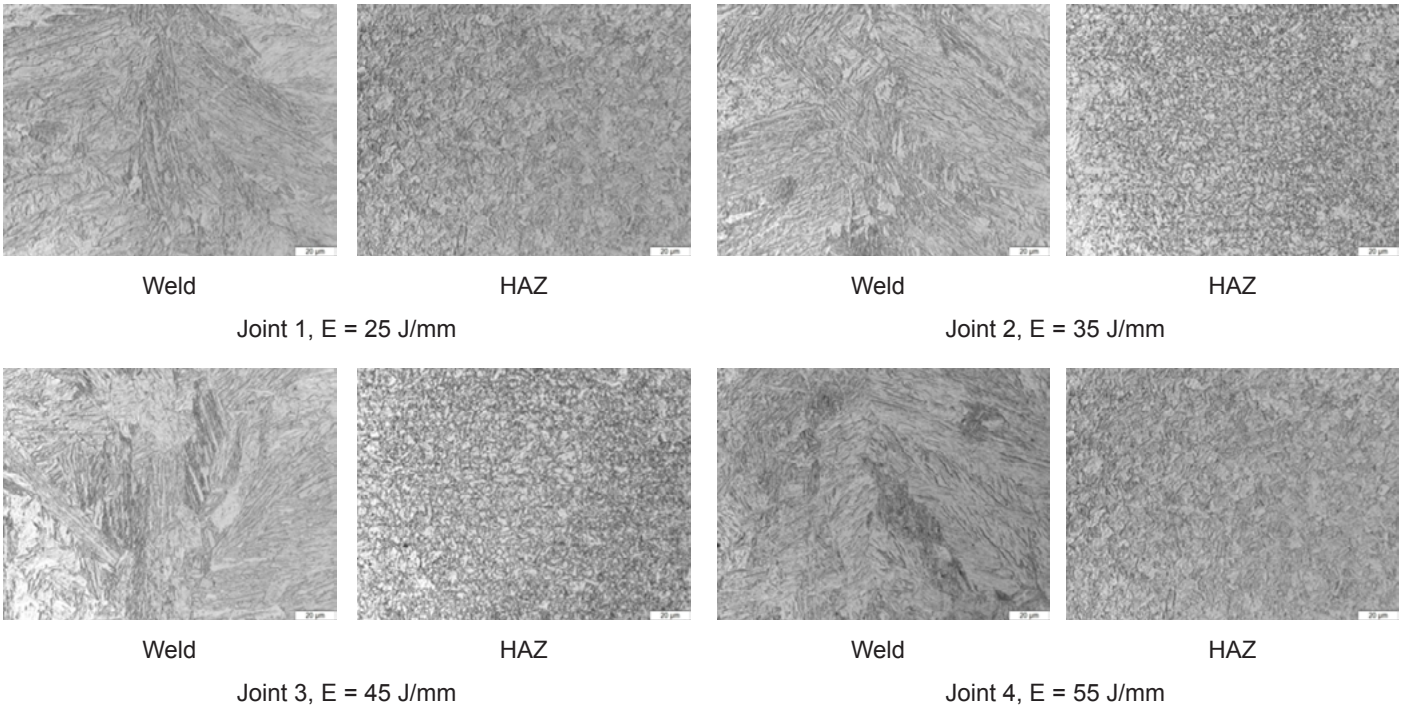

Weld | HAZ | Weld | HAZ

Joint 1, E = 25 J/mm | Joint 2, E = 35 J/mm

Weld | HAZ | Weld | HAZ

Joint 3, E = 45 J/mm | Joint 4, E = 55 J/mm

Fig. 4. Microstructure of the welded joints

Table 3. Tests results concerning the mechanical properties of the welded joints

Tensile strength *		**Bend test*, bend angle, °**	
R_m, MPa	Area of rupture	Weld face side	Weld root side
Joint 1; E = 25 J/mm			
1240	Base material	68	69
Joint 2; E = 35 J/mm			
1200	Fusion line	66	72
Joint 3; E = 45 J/mm			
1150	HAZ	84	83
Joint 4; E = 55 J/mm			
1120	HAZ	140	138
* average result based on two measurements			

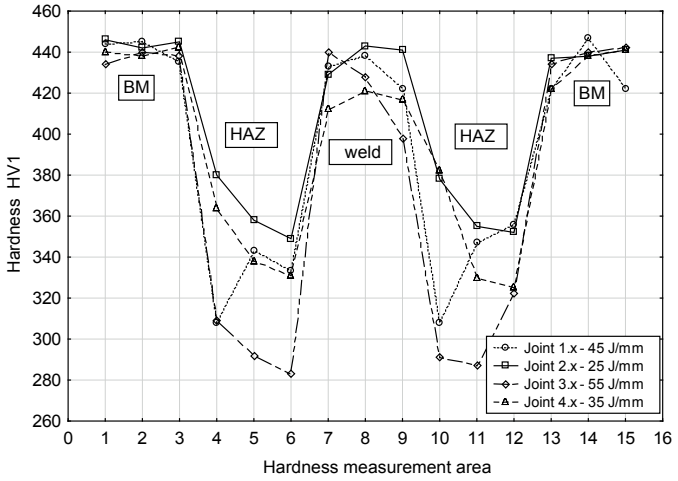

Fig. 5. Hardness distribution in the welded joints

Corrosion tests of welded joints

The objective of the gravimetric method-based corrosion tests was to determine the corrosion resistance of the welded joints in alkaline, inert and acidic environments. The specimens were first weighed using an analytical balance, degreased, and measured and, subsequently, immersed in the 0.1M solution of sodium hydroxide (NaOH), the 3.5% solution of sodium chloride (NaCl) and in the 0.1M solution of sulphuric acid (VI) – H_2SO_4. The proportion of liquid volume (expressed in cubic centimetres) to the area of the specimen (expressed in square centimetres) was 10:1. After 7 days, the specimens, previously subjected to cleaning, were weighed again to determine mass decrement V_c (formula (1)). The subsequent stage involved the calculation of corrosion linear rate V_p, (formulas (2, 3)):

$$V_c = \frac{\Delta G}{At} \quad (1)$$

where
V_c – mass decrement [g/m²day],
ΔG – change of the specimen mass [g],
A – active surface of the specimen before the test [m²],
t – test duration [days (24 hours)].

$$V_p = V_C \alpha \quad (2)$$

$$\alpha = \frac{365}{1000d} \quad (3)$$

where
V_p – linear corrosion rate [mm/year],
α – coefficient correlating the specimen mass decrement and the linear corrosion rate,
d – material density [g/cm3].

The gravimetric tests were followed by fractographic tests aimed to identify the type and nature of corrosion-triggered damage. The fractographic tests involved the use of a SteREO Discovery V12 stereoscopic microscope (Zeiss). Exemplary results are presented in Figure 6.

Analysis of test results

The non-destructive tests made it possible to classify the joints as representing quality level B in accordance with the ISO 13919 standard. The tests of mechanical properties revealed the possibility of making joints characterised by strength equal or similar to that of the base

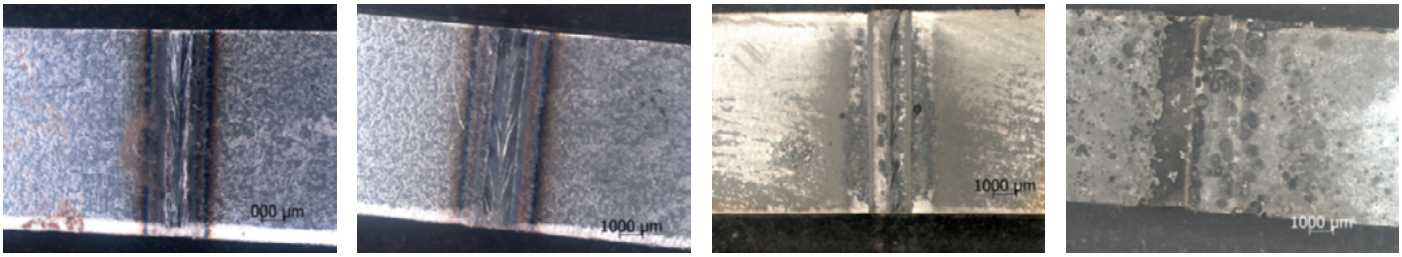

Joint 1, E = 25 J/mm | Joint 2, E = 35 J/mm | Joint 3, E = 45 J/mm | Joint 4, E = 55 J/mm

Fig. 6. Macrostructure of the welded joints after the corrosion tests

material. In terms of the joints welded using a linear energy of 25 J/mm, the rupture took place in the base material. As regards the remaining joints, the rupture took place in the fusion line or in the HAZ. An increase in welding linear energy was accompanied by an increase in the bend angle from 70° to 140°. The hardness measurements revealed that the weld was characterised by hardness similar to that of the base material. In turn, in the HAZ, an increase in welding linear energy was accompanied by a decrease in hardness, which could be ascribed to tempering processes.

The average results of corrosion linear rate Vp (Table 4) and of corrosion resistance (in accordance with the PN-55/H-04608 standard (Table 5)) were used to identify corrosion resistance groups (Table 6).

In the inert environment (3.5% solution of NaCl), the specimens corroded uniformly as a result of the reaction of the material with an aggressive component of the environment, i.e. chloride ions (Cl^-). The entire surface contained anodic and cathodic areas, where uniformly corroding specimens were mixed electrodes constituting shorted corrosion centres. The

Table 4. Test results concerning linear corrosion rate V_p [mm/year]

Joint no.	NaCl	NaOH	H_2SO_4
Joint 1, E = 25 J/mm			
Specimen 1	0.045911	0.001425	2.375142
Specimen 2	0.037177	0.002804	3.369719
Specimen 3	0.028497	0.002777	4.119999
Average	0.037195	0.002335	3.288287
Joint 2, E = 35 J/mm			
Specimen 1	0.066063	0.002952	3.705565
Specimen 2	0.041643	0.001495	4.355313
Specimen 3	0.038721	0.001448	3.954951
Average	0.048809	0.001965	4.005272
Joint 3, E = 45 J/mm			
Specimen 1	0.047457	0.003332	1.706086
Specimen 2	0.028519	0.001541	2.099836
Specimen 3	0.029674	0.003022	2.015978
Average	0.035217	0.002632	1.940634
Joint 4, E = 55 J/mm			
Specimen 1	0.009192	0.001297	1.929566
Specimen 2	0.033419	0.001325	1.367087
Specimen 3	0.002596	0.002594	1.471614
Average	0.015069	0.001739	1.589422

Table 5. Corrosion resistance in accordance with PN-55/H-04608

Determination of corrosion resistance group	Designation	Corrosion resistance degree	Linear corrosion rate V_p [mm/year]
Entirely resistant	I	1	below 0,001
Very resistant	II	2	above 0.001 up to 0.005
		3	above 0.005 up to 0.01
Resistant	III	4	above 0.01 up to 0.05
		5	above 0.05 up to 0.1
Less resistant	IV	6	above 0.1 up to 0.5
		7	above 0.5 up to 1.0
Slightly resistant	V	8	above 1.0 up to 5.0
		9	above 5.0 up to 10.0
Not resistant	VI	10	above 10

Table 6. Determination of corrosion resistance groups on the basis of corrosion rate V_p

	Determination of corrosion resistance group	Designation	Corrosion resistance degree
NaCl – inert	Resistant	III	5
NaOH – alkaline	Very resistant	II	2
H_2SO_4 – acidic	Slightly resistant	V	8

corrosion products were only slightly bounded with the base material and did not provide a sufficient protective barrier restricting corrosion processes. The weld area contained numerous, yet small-sized and variously shaped corrosion pits, the diameter of which was probably smaller than their depth. With the passage of time, the pits developed faster as a result of autoacceleration; inside the pits the concentration of halide ions (Cl^-) increased, whereas that of oxygen decreased.

In the alkaline environment it was possible to observe that the most intense corrosion process occurred in the heat affected zone. The steel surface corroded uniformly (additionally), yet the corrosion products significantly slowed down anodic processes. Metallographic observations correlated with the results obtained in the gravimetric method-based tests. The specimens exposed to the 0.1 M solution of NaOH were characterised by the smallest mass decrement and, consequently, the lowest linear corrosion rate. As a result, the test material could be regarded as belonging to the group of very resistant materials when exposed to an alkaline environment.

The most intense corrosion process took place in the acidic environment, which resulted from the fast depolarisation of oxygen and the release of hydrogen. The layer of iron oxide dissolved in the environment characterised by low pH, the result of which was the direct contact of iron with the solution. The metallographic observations revealed the significant corrosion-triggered damage to the material, characterised by the presence of swells and pits across the entire surface area. It was also possible to notice significant material losses and cracks.

Conclusions

The above-presented tests of the 1.8 mm thick laser welded joints made of steel Docol 1200M revealed the possibility of making joints satisfying the criterial specified in the ISO 15614-11 standard. In spite of the high carbon equivalent of steel AHSS Docol 1200M, it was possible to obtain laser welded joints without

compromising high mechanical properties. The weld area of all of the joints contained acicular martensitic structure characterised by variable sizes of aciculae (depending on supplied energy). An increase in welding linear energy was accompanied by an increase in the size of martensite aciculae. In the HAZ, the base material underwent tempering, which led to the formation of the softened zone. Steel Docol 1200M was characterised by the highest corrosion resistance in the alkaline solution and by the lowest corrosion resistance in the acidic solution. The gravimetric method is a very good and simple solution making it possible to determine the rate of uniform corrosion over a long period. The material subjected to analysis was characterised by varied environment-related corrosion resistance. Corrosion-triggered damage observed in the joints included cracks, pits, swells and losses.

References

[1] Lee C., Shin H., Park K.: Evaluation of high strength TMCP steel weld for use in cold regions. Journal of Constructional Steel Research, 2012, no. 74. pp. 134–139.

[2] Yurioka N.: TMCP steels and their welding. Welding in the World, 1995, no. 35/6, pp. 375–390.

[3] Górka J.: Weldability of thermomechanically treated steels having a high yield point. Archives of Metallurgy and Materials, 2015, vol. 60, no. 1, pp. 469–475, doi: 10.1515/amm-2015-0076.

[4] Lisiecki A.: Welding of Thermomechanically Rolled Fine-Grain Steel by Different Types of Lasers. Archives of Metallurgy and Materials, 2014, vol. 59, pp. 1625–1631, doi: 10.2478/amm-2014-0276.

[5] Opiela M.: Effect of Thermomechanical Processing on the Microstructure and Mechanical Properties of Nb-Ti-V Microalloyed Steel. Journal of Materials Engineering and Performance, 2014, no. 9, pp. 3379–3388.

[6] Janicki D.: Fiber laser welding of nickel based superalloy Rene 77, Proceedings of SPIE, vol. 8703, Laser Technology 2012: Applications of Lasers, 87030S, 2013, doi: 10.1117/12.2013428.

[7] Lisiecki A.: Effect of heat input during disk laser bead-on-plate welding of thermomechanically rolled steel on penetration characteristics and porosity formation in the weld metal. Archives of Metallurgy and Materials, 2016, no. 61, pp. 93–102, doi: 10.1515/amm-2016-0019.

[8] Kurc-Lisiecka A. et al.: Analysis of deformation texture in AISI 304 steel sheets, Solid State Phenomena, 2013, no. 203–204, pp. 105–110, doi: 10.4028/www.scientific.net/SSP.203-204.105.

[9] Grajcar A., Różański M., Stano S., Kowalski A.: Microstructure characterization of laser-welded Nb-microalloyed silicon-aluminum TRIP steel. Journal of Materials Engineering and Performance, 2014, vol. 23, no. 9, pp. 3400–3406.

[10] Lisiecki A.: Welding of titanium alloy by disk laser, Proc. of SPIE, vol. 8703, Laser Technology 2012: Applications of Lasers, 87030T (2013), doi: 10.1117/12.2013431.

[11] Grajcar A., Różański M., Kamińska M., Grzegorczyk B.: Study on Non-Metallic Inclusions in Laser-Welded TRIP-Aided Nb-Microalloyed Steel. Archives of Metallurgy and Materials, 2014, no. 59, pp. 1163–1169, doi: 10.2478/amm-2014-0203.

[12] Janicki D.: Disk laser welding of armour steel. Archives of Metallurgy and Materials, 2014, vol. 59, pp. 1641–1646, doi: 10.2478/amm-2014-0279.

[13] Górka J.: Study of structural changes in S700MC steel thermomechanically treated under the influence of simulated welding thermal cycles. Indian Journal of Engineering and Materials Sciences, 2015, no. 22, pp. 497–502.

[14] Żuk M., Górka J., Czupryński A., Adamiak M.: Properties and structure of the

weld joints of quench and tempered 4330V steel. Metalurgija, 2016, vol. 55, no. 4, pp. 613–616.
[15] Grajcar A., Różański M., Stano S.: Effect of heat input on microstructure and hardness distribution of laser welded Si-Al TRIP-type steel. Advances Material Science Engineering. 2014. Article ID 658947, pp. 1–8.
[16] Charleux M., Poole W.-J., Militzer M.: Precipitation behavior and its effect on strengthening of an HSLA-Nb/Ti steel. Metallurgical and Materials Transactions A, 2001, no. 32, pp. 1635–1647.
[17] Górka J.: Analysis of simulated welding thermal cycles S700MC using a thermal imaging camera. Advanced Material Research, 2014, 1036, pp. 111–116.
[18] Stano S.: Spawanie laserowe blach o zróżnicowanej grubości przeznaczonych na półfabrykaty karoserii samochodowych typu tailored blanks. Biuletyn Instytutu Spawalnictwa, 2005, no. 2, pp. 24–28.